RESEARCH PAPER

Evaluation of mechanical properties of PEEK-LT3+nHA Composites for Biological applications by using 3D printing technology

Moinuddin S K[1], Syed Zameer[2], Sudhakar Koppa Hanumanthe Gowda[3], Ashwin Balur Narayana[4], Sanjay Bhat[5], Mohammed Mohsin Ali H[6]

[1]Assistant Professor, Department of Mechanical Engineering, Ghousia College of Engineering, Ramanagaram, Karnataka 562159, India, Affiliated to VTU Belagavi.

[2]Associate Professor, Department of Mechanical Engineering, Ghousia College of Engineering, Ramanagaram, Karnataka562159 , India.

[6]Associate Professor, Department of Mechanical Engineering, Ghousia College of Engineering, Ramanagaram, Karnataka562159 , India

***Correspondence:** moinuddinsk88@gmail.com, sudhakarkh@gmail.com, bnashwin87@gmail.com, Sanjaybhattre@gmail.com.

ABSTRACT

This study investigates the mechanical and micro structural behaviour of 3D-printed PEEK-LT3/nano-hydroxyapatite (nHA) composites fabricated using Fused Deposition Modelling (FDM). Composites containing 0 wt.%, 3 wt.%, 6 wt.%, and 9 wt.% nHA were developed and evaluated through tensile, impact, hardness, optical microscopy, and SEM analysis. The results showed significant improvement in mechanical properties with the addition of nHA reinforcement. The tensile strength increased from 174.6 MPa for pure PEEK-LT3 to a maximum of 277.66 MPa at 6 wt.% nHA, while the impact strength improved from 32 kJ/m² to 44.5 kJ/m². The hardness continuously increased from 55 VHN to 81 VHN with increasing nHA content. SEM and micro structural observations revealed improved particle dispersion, interfacial bonding, and reduced porosity at optimum reinforcement levels. However, excessive reinforcement at 9 wt. % nHA caused particle agglomeration and slight reduction in tensile and impact properties. The study concludes that 6 wt. % nHA provides the best combination of strength, toughness, and structural integrity, making the developed composite suitable for biomedical and advanced engineering applications.

Keywords: PEEK-LT3 (Polyetheretherketone), nHA (nano Hydroxyapatite), Polymer Composites, Additive Manufacturing, Mechanical Properties, SEM

How to cite this article: Moinuddin SK, Zameer S, Gowda SKH, Narayana AB, Bhat S, Ali MMH. Evaluation of mechanical properties of PEEK-LT3+nHA Composites for Biological applications by using 3D printing technology. Int J Drug Deliv Technol. 2026;16(57s): 935-951. DOI: 10.25258/ijddt.16.57s.99

Source of support: Nil

Conflict of interest: None

1. INTRODUCTION

3D printing provides the possibility of low volume and cost effect production as well customized parts with extraordinary features such as multilateral fabrication, light weight hollow material and fabrication of complex structure which are not possible using traditional fabrication techniques such as CNC milling, casting or moulding [7]. Material information is not widely available in 3D printing due to the fact that the wide range of printing parameter combinations (infill %, layer thickness, infill pattern, speed, temperature) lead to very different outcomes [5]. Material properties will change depending on setting used within the printer. Determining the effect of process parameters is also an important aspect of this project, as it will improve knowledge about optimal settings and assist users in the correct selection of process parameters in real world applications [11].

1.1 3D PRINTING OVERVIEW

3D printing, also referred to as additive manufacturing (AM), rapid prototyping (RP), or solid free form fabrication (SFF), is the fabrication of objects through the deposition of a material, layer by layer using a print head, or nozzle, to make objects from 3D model data [1]. As Part of the 4th industrial revolution, Additive

Manufacturing (or 3D-Printing) holds extraordinary potential. Dating back to the 1980's, the technology began to prototype new designs quickly and efficiently. For the following two decades, it developed as a niche technology with limited applicability, until new developments opened its potential to more serious applications [9] [10]. Today Medical uses for 3D printing include: tissue and organ fabrication; creation of customized prosthetics, implants, and anatomical models; and pharmaceutical research regarding drug dosage forms, and delivery [2]. 3D printers for biomedical applications are one of the current growth leaders within the market [3]. In 2014 the majority of 3D printers sold for use in the medical devices industry were based on material jetting and photo polymerization techniques where polymer based printing accounted for the majority of materials used in the market [3]. Fused deposition modelling (FDM) was first developed by Scott Crump in 1989 [11]. It is one of the most widely used AM techniques. This is due to the availability of FDM printers also known as rep rap printers for both industrial and public use becoming affordable and widely available in a newly competitive market. 3D printers have verified their use in a wide range of applications for prototyping and engineering [12], customizing scientific equipment [13] and appropriate technology-related product manufacturing for sustainable development.

Recent advances and uses in 3D printing include 3D-printed patches infused with endothelial cells which are being used to treat Ischemia [14], a 3D Bio pen used to repair cartilage and bone whereby the pen is loaded with a bio-ink comprised of stem cells inside a biopolymer which is in turn protected by a second layer of hydrogel. The ink is then extruded onto the bone surface and solidified by a UV light embedded in the pen [15]. Materials used for printing include, ABS, PC and PLA [16]. Unlike ABS or PC, PLA is an environmentally friendly biodegradable polymer. PLA has been used in clinical applications for years and has been proven to be biocompatible and safe to use in vivo [[19]. It is evident that there is a need to thoroughly evaluate the properties of PLA components produced via FDM, for use in FEA analysis, so that they may continue to be successfully used for both industrial and general use. Furthermore, the use of FEA analysis will enable a greater understanding of how a 3D-printed part will perform in the physical world and it is an area that is developing to meet the needs of the additive manufacturing market [6].

1.2 FUSED DEPOSITION MODELLING (FDM).

It begins with a meshed 3D computer model that can be created by acquired image data or structures built in computer-aided design (CAD) software. A Stereo lithography (STL) file is created and the mesh data will be further sliced into a build file of 2D layers and sent to the 3D printing machine where the part is printed. FDM uses preformed polymer filament that is supplied on a spool as the building material.

The PEEK-LT3 filament is fed to a fine print head or nozzle which melts and extrudes it [3] [20]. The extrusion temperature can be varied to suit the material that is being used. The nozzle, being free to move in the x, y and z axis, builds the 3D structure by injecting the melt onto a base plate and building its way up as the parts cure naturally [7]. As a natural consequence of this manufacturing approach, parts fabricated using FDM exhibit anisotropic properties. This implies that determination of the build strategy will have a pronounced effect on the properties and ultimately the performance of the part [21].

PEEK-LT3 is an aliphatic polyester thermoplastic derived from starches of corn and sugarcane. PEEK-LT3 is immunologically inert as it gradually degrades into harmless this makes it attractive for use in the field of medicine. Additionally, PEEK-LT3 has a high glass transition temperature (Tg = 257–300 oC) and melting temperature (Tm = 380–396 oC), Since the melting temperature is very high only on specialized type of 3D printing machines with high nozzle temperature can be used to print the samples. A study by Cuiffo et al 2017 investigated the effect of the FDM printing process on the chemistry and structure of PEEK-LT3. It was found through extensive investigation that heating, melting, and recrystallization of the PEEK-LT3 as a function of the printing process has drastically changed the nature of the PEEK-LT3, making it stronger (via tensile testing measurements) and more chemically reactive. The FDM printing process results in changes to the structure of the PEEK-LT3, which is reflected in shifts in the temperature range and potential mechanism of cold crystallization, as well as the resulting melting characteristics [22]. Furthermore Drummer et al. 2012 [18] examined the material behavior of PEEK-LT3 during processing by FDM and the resulting part properties. Samples were printed at three different nozzle temperatures to determine the influence of the processing temperature and to evaluate using short-term tensile testing.

2. MATERIALS AND METHODS.

2.1 Fused Deposition Modelling.

Fused deposition modelling (FDM) is an advanced 3D printing technique for the manufacture of plastic materials. The ease of use, prototyping accuracy and low cost makes it a widely used additive manufacturing technique. FDM creates 3D structures through the layer-by-layer melt extrusion of a plastic filament. The production of a printed structure involves the generation of a digital design of the model by 3D design software and its execution by the printer until the complete model is reproduced. This review presents the current status of FDM, how to handle and operate FDM printers, industry

standards of printing, the types of filaments that can be used, the post-processing treatments, advantages, and limitations as well as an overview of the increasing application fields of FDM technology. The application areas of FDM are endless, including biomedicine, construction, automotive, aerospace, acoustics, textiles, and occupational therapy amongst others. Even during the current Corona virus disease (COVID19) pandemic, FDM has helped to fabricate face masks, ventilators and respiratory systems, respiratory valves, and nasopharyngeal swabs for COVID-19 diagnosis. FDM 3D and 4D printing can produce polymeric and composite structures of various designs, and compositions in a range of materials according to the desired application. The review concludes by discussing the future prospects for FDM.

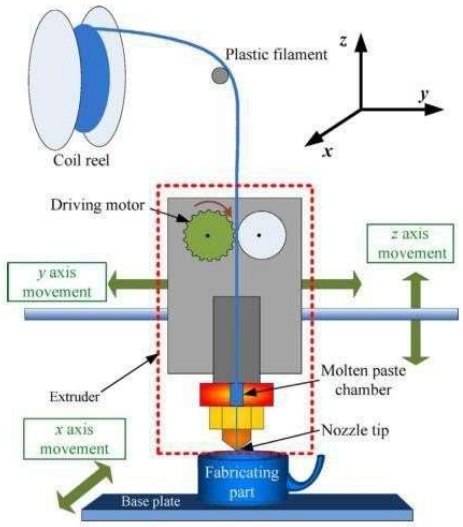

Fig. 2.1 Fused Deposition Modeling.

2.2 Basic concepts of Fused Deposition Modelling.

2.2.1 Main stages

As a general scheme, the core principle of the FDM production method is simply to melt the raw material and facilitate the creation of new shapes. The material is made of a filament coil on a wheel that is driven into a temperature-controlled nozzle which heats it to a semiliquid. The nozzle accurately extrudes and guides the molten material to build a structural element layer by layer. This replicates the outlines of a layer that has been introduced into the FDM working system by the application program. FDM begins with the virtual design of the part to be printed which is generated using a computer-aided design (CAD) software in a ".stl" format. Some of the most popular software packages used to produce this type of files are AutoCAD, Free CAD, Autodesk Inventor, Solid Works or Tinker cad. The ".STL" file is processed by a slicing or laminating program which converts the design into printer-specific instructions so that the printer can "understand" the design. The ".stl" file is transformed into a ".gcode" file. The specifications necessary to be able to print the part, such as print speed, size of the print thread, temperature and layer height are selected in a slicer or slicing program such as Slic3r and Cura. These programs produce a file with ".gcode" format, which can be directly read by the printer to print the design [75]. The G-code is the most broadly used computer numerical control (CNC) programming language that is used in computer aided manufacturing to control automated machine tools including 3D printers [76]. Figure 1 shows a general summary of the FDM process.

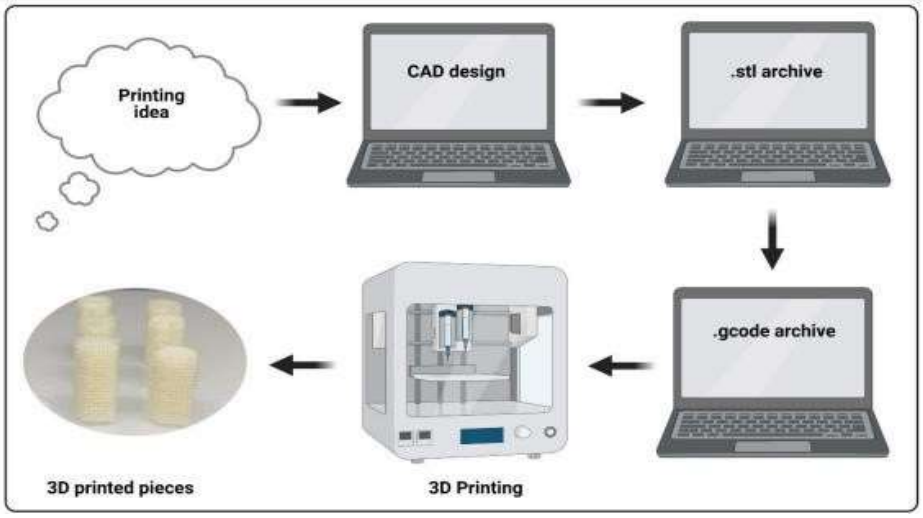

Fig. 2.2 General summary of the FDM process.

2.3 3D PRINTED TEST SPECIMENS

Dog bone type specimens seen in Figure 7 were prepared according to the geometry and dimensions specified in D638 – 14 Standard Test Method for Tensile Properties of Plastics [27]. The dog-bone specimen was designed using Solid works 2016 and thus it was exported in an STL format. This is the file format that can be imported to slicer, the program used by the Original Prusa i3 MK2 3D Printer to slice the part, design the road tool path and then send the related commands to the 3D Printer. See Appendix A for fully dimensioned drawing. Studies which have examined the mechanical properties of 3D printed polymer parts have shown to apply the same methodology for preparing a test piece for 3D printing. The specimen conforming to ASTM D638 is drawn in CAD and the file is then exported to the printer as an STL file [10], [21], [24]–[26].

Test specimen size: The ASTM D-3039 [27] standard provides five individual test coupon dimensions (Types I through V) for the determination of tensile properties of plastics. Figure 3 illustrates ASTM Tensile Test Specimens Type I. The standard specifies the preference for Type I specimens over the alternatives, however it does not directly specify a recommended type to be used in the evaluation of parts fabricated through FDM technology [27]. ASTM/ISO protocols have not been established for testing of 3D printed polymer parts, existing methods provide guidelines to establish the fractural and tensile properties of PLA FDM components [25].

The tensile strength is the maximum tensile stress of the material and can be found by applying equation:

Stress=F/A

Where: F= applied Force(N)

A=cross section area (mm2)

The test process involves placing the test specimen in the testing machine and applying tension to it until it fractures. During the application of tension, the elongation of the gauge section is recorded against the applied force. The data is manipulated so that it is not specific to the geometry of the test sample. The elongation measurement is used to calculate the *engineering strain*, ε, using the following equation:

$$\varepsilon = \frac{\Delta L}{L_0} = \frac{L - L_0}{L_0}$$

where ΔL is the change in gauge length, $L0$ is the initial gauge length, and L is the final length. The force measurement is used to calculate the *engineering stress*, σ, using the following equation:

$$\sigma = \frac{F_n}{A}$$

Where F is the force and A is the cross-section of the gauge section. The machine does these calculations as the force increases, so that the data points can be graphed into a stress- strain curve. Tensile test is performed to determine certain mechanical properties.

A specifically prepared sample is placed in the heads of the testing machine and an axial load is placed on the sample through a hydraulic or mechanical loading system. The force is

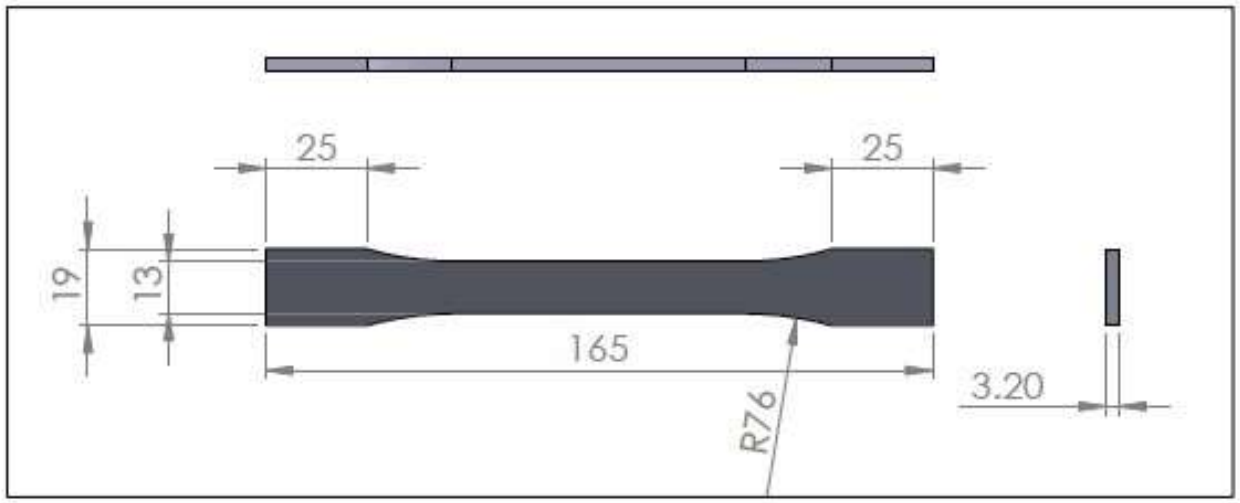

Fig 2.3 ASTM Standard D-3039 Tensile Test Specimen.

2.4 PRINTING OF TENSILE SPECIMENS.

Printing of the tensile and specimens was carried out on an Original Prusa i3 MK2 3D printer which can be seen below in Figure 12. The printing material used was 1.75 mm PLA filament. Each specimen was printed individually with a print time of between 20 minutes to 60 minutes depending on print run settings.

Fig. 2.4. High-temperature FDM 3D printer used for PEEK-based filament fabrication..

A print time of approximately 100 hours was needed to complete printing of all specimens. Tensile testing to evaluate the mechanical properties of each specimen was carried out on an Tinius Olsen H2K5S. A 10KN load cell was used with an extensometer with a gauge length of 50mm. Speed of testing was determined using ASTM D638 Standard Test Method for Tensile Properties of Plastics [27]. A speed of 5.00 mm/min (in./min) was used as it is the recommended speed for type I test samples

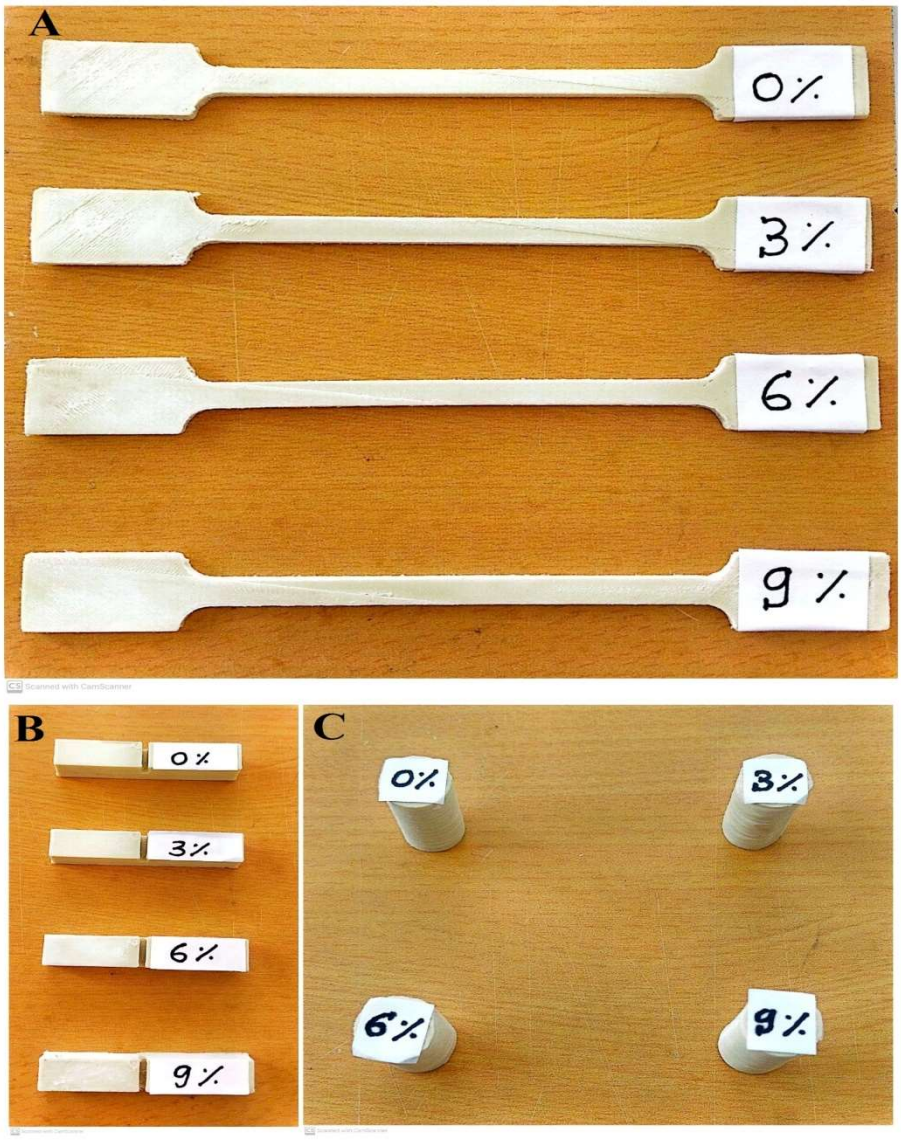

Fig. 2.5 Tensile specimens of PEEK-LT3 Composites

2.5 Mechanical Tests.

2.5.1. Tensile testing

Fig. 2.6 Tensile Test Machine.

Tensile testing to evaluate the mechanical properties of each specimen was carried out on an

Tinius Olsen H2K5S. A 10Kn load cell was used with an extensometer with a gauge length of 50mm. Speed of testing was determined using ASTM D638 Standard Test Method for Tensile Properties of Plastic [27]. A speed of 5.00 mm/min (in./min) was used as it is the recommended speed for type I test samples.

2.5.2 Scanning Electron Microscope (SEM)

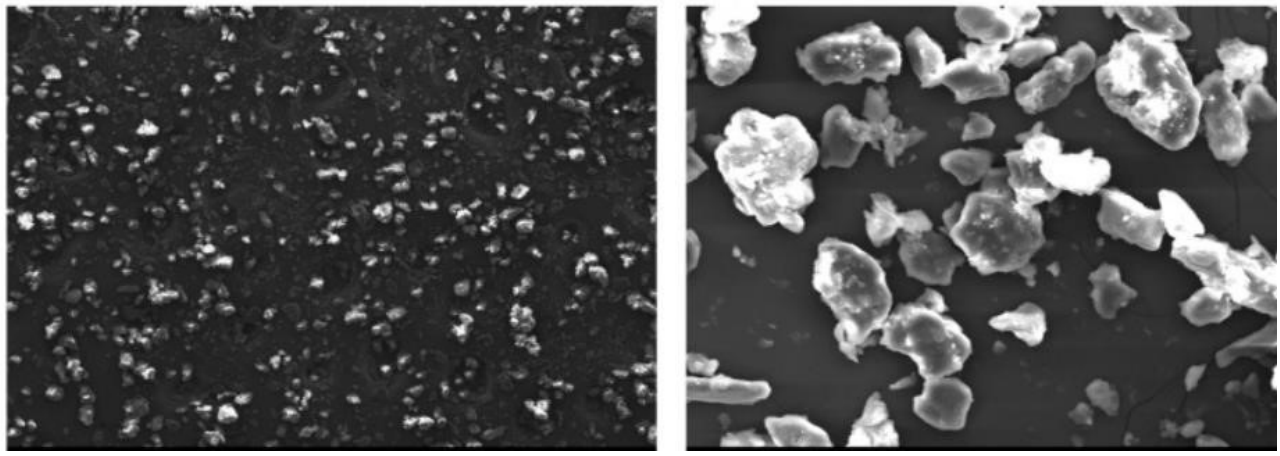

Fig. 2.7 Scanning Electron Microscope Images (SEM)

A Scanning Electron Microscope (SEM) is a type of electron that produces images of a sample by scanning the surface with a focused beam of electrons The electrons interact with atoms in the sample, producing various signals that contain information about the surface topography and composition of the sample. The electron beam is scanned in arrester scan pattern, and the position of the beam is combined with the intensity of the detected signal to produce an image. In the most common SEM mode, secondary electrons emitted by atoms excited by the electron beam are detected using a secondary electron detector (Everhart– Thornley detector).

Fig. 2.8 Scanning Electron Microscope (SEM)

2.5.4. Hardness.

Hardness is the property of the material that enables to resist plastic deformation, usually by penetration. However, the term hardness may also refer to resistance to bending, scratching, abrasion or cutting. Hardness is not an intrinsic material property dictated by precise definitions in terms of fundamental units of mass, length and time. A hardness property value is the result of a defined measurement procedure. Hardness of materials has probably long been assessed by resistance to scratching or cutting. In general, addition of hard reinforcement in the matrix alloy results in improved

hardness of composites [8]. Presence of soft reinforcement in the matrix alloy reduces the hardness of the obtained composites. The type and extent of incorporation of the reinforcement has a influence on the hardness of the composite. The hardness of the composite depends on the nature of the reinforcement present and also on the quantity of the reinforcement. Further improvement in hardness can be obtained by heat treatment.

2.5.5 Micro - Hardness.

The microstructures of both with heat treated and without heat treated specimens were grinded on the Silicon Carbide abrasive paper of 300, 600, 800, 1000, & 1200 grit sizes. The grinding was done in successive steps on each abrasive paper. After emery polishing, the specimens were thoroughly washed, dried and polished on a double disc polishing machine. Fig.4.8 shows the double disc polishing machine.

Fig.2.9 Double Disc Polishing Machine

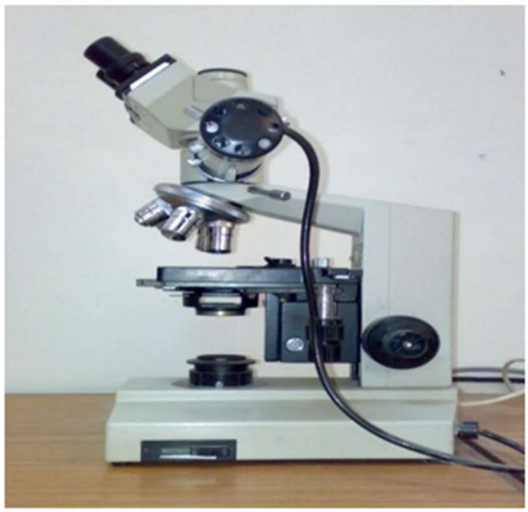

Fig. 2.10 Optical Metallurgical Microscope

3. RESULTS AND DISCUSSION.

3.1 TENSILE TEST:

Table 01: Tensile Strength of PEEK-LT3 and nHA Strength

SPECIMEN	Tensile stress in Mpa
PEEK-LT3-0%Wt nHA	174.60
PEEK-LT3-3%Wt nHA	239.36
PEEK-LT3-6%Wt nHA	277.66
PEEK-LT3-9%Wt nHA	266.84

Fig 3.1. The influence of NHA on Tensile

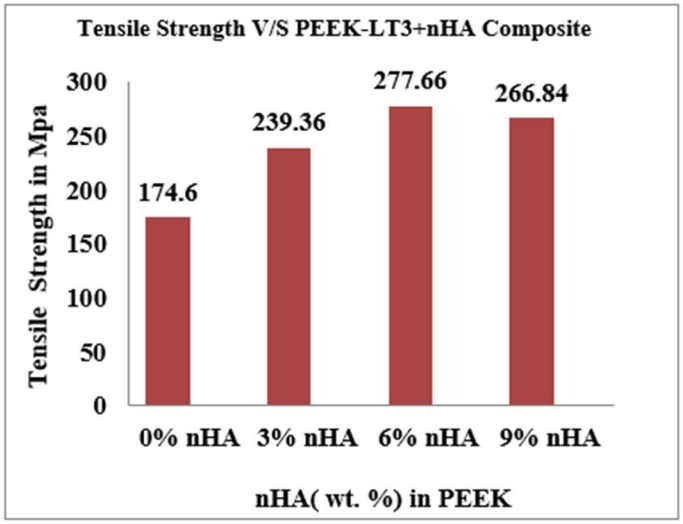

The graph presents the variation in tensile strength of the PEEK-LT3 composite with different concentrations of nano-hydroxyapatite (nHA) reinforcement. Tensile strength is a critical mechanical property that indicates the maximum stress a material can withstand before fracture under tensile loading conditions. From the graph, it is evident that the incorporation of nano-hydroxyapatite significantly improves the tensile strength of the

composite up to an optimum filler concentration, after which a slight reduction is observed [33-37]. This trend demonstrates the important role of nHA reinforcement in enhancing the load-bearing capability and structural integrity of the PEEK composite. The unreinforced PEEK-LT3 composite containing 0 wt.% nHA exhibits a tensile strength of 174.6 MPa, which serves as the baseline mechanical performance of the material. In the absence of reinforcement particles, the polymer matrix alone resists the applied tensile forces. Although PEEK inherently possesses good mechanical strength and toughness, the lack of reinforcing fillers limits its resistance to crack propagation and deformation under high tensile stress.Upon the addition of 3 wt.% nHA, the tensile strength increases substantially to 239.36 MPa**.** This considerable improvement indicates that even a small amount of nano-hydroxyapatite effectively strengthens the composite structure. The enhancement in tensile strength can be attributed to the uniform dispersion of nHA particles within the PEEK matrix and the improved interfacial bonding between the reinforcement and polymer phases. The nanoparticles act as stress-transfer agents, enabling the applied load to be distributed more efficiently throughout the composite. Furthermore, the presence of nHA particles restricts the mobility of polymer chains and inhibits crack initiation, thereby improving the resistance of the material to tensile failure. The maximum tensile strength of 277.66 MPa is achieved at 6 wt.% nHA, indicating that this composition provides the optimum reinforcement effect. At this concentration, the nanoparticles are likely to be well dispersed and strongly bonded to the matrix, resulting in highly effective stress transfer between the PEEK matrix and the ceramic reinforcement [4-7]. The strong interfacial adhesion enhances the ability of the composite to withstand higher tensile loads before fracture. In addition, the well dispersed nanoparticles contribute to crack deflection and crack bridging mechanisms, which delay crack propagation and improve the overall mechanical performance. Compared to the unreinforced composite, the tensile strength at 6 wt. % nHA shows a remarkable increase, demonstrating the significant reinforcing capability of nano-hydroxyapatite. However, when the nHA content is further increased to 9 wt.%**,** the tensile strength slightly decreases to 266.84 MPa. Although the tensile strength remains considerably higher than that of pure PEEK-LT3, the reduction compared to the 6 wt.% composition suggests that excessive addition of nano-hydroxyapatite adversely affects the composite performance. At higher filler concentrations, nanoparticles tend to agglomerate due to their large surface area and high surface energy. These agglomerated regions create stress concentration sites within the matrix, which may initiate microcracks during tensile loading. Moreover, excessive ceramic reinforcement reduces the ductility and flexibility of the polymer matrix, causing the material to become relatively brittle. As a result, the tensile strength decreases slightly beyond the optimum reinforcement level. Overall, the graph clearly demonstrates that the addition of nano-hydroxyapatite significantly enhances the tensile strength of PEEK-LT3 composites up to an optimum concentration of 6 wt.% nHA. The improvement in mechanical performance is primarily due to enhanced interfacial bonding, efficient stress transfer, restricted polymer chain movement, and improved crack resistance provided by the uniformly dispersed nanoparticles [40]. The slight decrease observed at higher filler loading is mainly associated with particle agglomeration and increased brittleness of the composite. Therefore, based on the obtained results, 6 wt.% nHA can be considered the optimum reinforcement concentration for achieving maximum tensile strength in the developed PEEK-LT3+nHA composite system.

3.2 Impact Strength.

The mechanical characterization of PEEK-LT3 and its carbon fiber reinforced composites reveals a contrasting behavior in tensile and impact strength with respect to reinforcement content. The tensile strength results showed a progressive improvement from 174.6 MPa for neat PEEK-LT3 to a peak of 277.66 MPa at 6% nHA, representing an enhancement of nearly 59%.

Table 02: Impact Strength of PEEK-LT3 and NHA

SPECIMEN	Impact Strength kJ/m^2
PEEK-LT3-0%Wt nHA	32
PEEK-LT3-3%Wt nHA	39.7
PEEK-LT3-6%Wt nHA	44.5
PEEK-LT3-9%Wt nHA	43

Fig 3.2. The influence of nHA on Tensile Strength

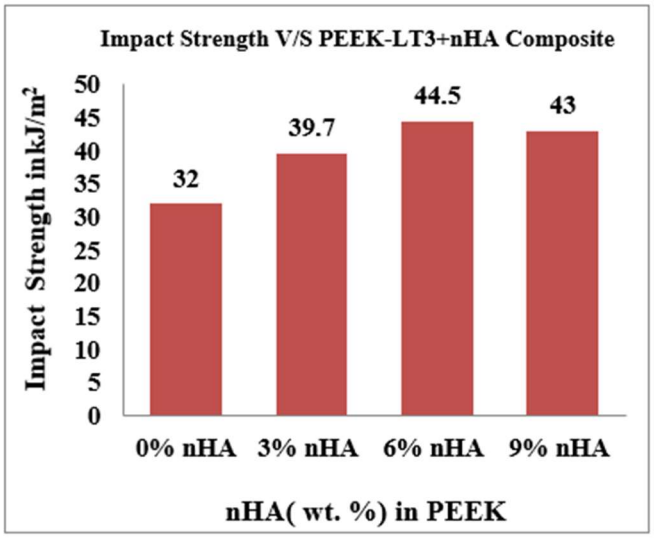

The graph illustrates the variation in impact strength of the 3D-printed PEEK-LT3 composites with different concentrations of nano-hydroxyapatite (nHA) reinforcement. Impact strength is an important mechanical property that represents the ability of a material to absorb sudden impact energy before fracture. The graph clearly shows that the impact strength of the composite increases progressively with the addition of nHA up to an optimum concentration and then exhibits a slight reduction at higher filler loading [28]. This trend indicates that both nano-hydroxyapatite reinforcement and the 3D-printing process significantly influence the toughness and energy absorption capability of the developed composite material. The pure 3D-printed PEEK-LT3 composite containing 0 wt.% nHA exhibits an impact strength of 32 kJ/m², which serves as the baseline value for comparison. In this condition, the material consists only of the polymer matrix fabricated through the 3D-printing process. Although PEEK possesses excellent inherent toughness and thermal stability, the absence of reinforcing particles limits its resistance to sudden impact loading. In additively manufactured components, factors such as interlayer bonding, raster orientation, layer adhesion, and printing temperature strongly influence the impact performance [19-26]. During 3D printing, incomplete fusion between adjacent deposited layers can create weak interfaces and microscopic voids, which may act as crack initiation sites under impact loading. As a result, the impact strength of the unreinforced composite remains comparatively lower. When 3 wt.% nHA is incorporated into the PEEK matrix, the impact strength increases significantly to 39.7 kJ/m². This improvement demonstrates that the addition of nano-hydroxyapatite effectively enhances the toughness of the composite. The increase in impact strength can be attributed to the uniform dispersion of nanoparticles within the polymer matrix and the improved interfacial interaction between PEEK and nHA. The nanoparticles act as reinforcement centers that absorb and redistribute impact energy more efficiently throughout the composite structure. Furthermore, the presence of well-dispersed nHA particles hinders crack initiation and propagation during sudden loading conditions. In the context of 3D printing, the nanoparticles may also improve the thermal conductivity and melt behavior of the composite during extrusion, leading to better interlayer diffusion and stronger bonding between printed layers. Improved interlayer adhesion contributes significantly to enhanced impact resistance in additively manufactured composites. The maximum impact strength of 44.5 kJ/m² is achieved at 6 wt.% nHA, indicating that this composition provides the optimum reinforcement effect for the 3D-printed PEEK-LT3 composite. At this concentration, the nanoparticles are likely to be uniformly distributed throughout the matrix, resulting in effective stress transfer and enhanced energy dissipation mechanisms [39-40]. The strong interfacial bonding between the PEEK matrix and nHA particles improves the ability of the composite to resist crack growth under impact loading. In addition, several toughening mechanisms such as crack deflection, crack pinning, and particle-matrix debonding contribute to higher energy absorption before failure. From the 3D-printing perspective, the optimized filler concentration may improve the fusion between deposited filaments, reduce internal porosity, and strengthen the layer-by-layer structure of the printed composite. Better interfacial fusion between printed layers minimizes weak regions and enables the material to withstand higher impact forces. Therefore, the combined effect of nanoparticle reinforcement and improved printing-induced

microstructure results in the highest impact strength at 6 wt.% nHA. However, when the nHA concentration is further increased to 9 wt.%, the impact strength slightly decreases to 43 kJ/m². Although the value remains higher than the unreinforced PEEK composite, the reduction compared to the 6 wt.% composition suggests that excessive filler loading negatively affects the toughness of the material. At higher concentrations, nano-hydroxyapatite particles tend to agglomerate due to their high surface energy, leading to non-uniform dispersion within the matrix. These agglomerated regions create stress concentration points that facilitate crack initiation under impact loading. Additionally, excessive ceramic filler reduces the ductility and flexibility of the polymer matrix, causing the composite to become relatively brittle. In 3D printing, higher filler content can also adversely affect the extrusion behaviour and flow ability of the material, leading to incomplete filament fusion, increased porosity, and weaker interlayer bonding. Such defects reduce the ability of the composite to absorb impact energy efficiently, resulting in a slight decline in impact strength at higher nHA loading. Overall, the graph demonstrates that the incorporation of nano-hydroxyapatite significantly enhances the impact strength of 3D-printed PEEK-LT3 composites up to an optimum concentration of 6 wt.% nHA. The improvement in impact performance is mainly attributed to enhanced interfacial bonding, efficient stress transfer, crack resistance mechanisms, and improved interlayer adhesion produced during the 3D-printing process. The slight decrease at higher filler loading is associated with particle agglomeration, increased brittleness, and possible printing-related defects such as poor filament fusion and void formation [7-11]. Therefore, based on the observed results, 6 wt.% nHA can be considered the optimum reinforcement concentration for achieving maximum impact strength and superior mechanical performance in the developed 3D-printed PEEK-LT3+nHA composite system.

3.3 Hardness

Table 03: Hardness of PEEK-LT3 and NHA

SPECIMEN	VHN
PEEK-LT3-0%Wt nHA	55
PEEK-LT3-3%Wt nHA	67
PEEK-LT3-6%Wt nHA	75
PEEK-LT3-9%Wt nHA	81

Fig 3.3. The influence of NHA on Vickers Hardness

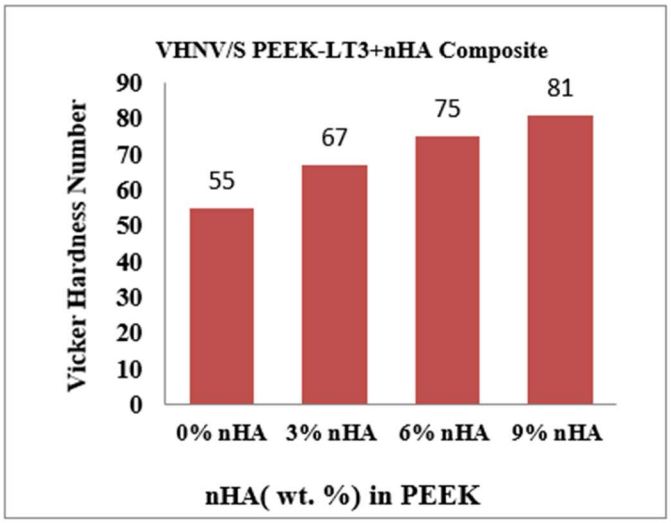

The graph illustrates the variation in Vickers Hardness Number (VHN) of the 3D-printed PEEK-LT3 composites with different concentrations of nano-hydroxyapatite (nHA) reinforcement. Hardness is an important mechanical property that indicates the resistance of a material to localized plastic deformation, indentation, scratching, and wear. From the graph, it can be clearly observed that the hardness of the composite increases continuously with increasing nHA content. This trend demonstrates that the incorporation of nano-hydroxyapatite significantly enhances the surface hardness and stiffness of the PEEK-based composite material[4]. The pure PEEK-LT3 composite without reinforcement, containing 0 wt. % nHA, exhibits a Vickers hardness value of 55 VHN**,** which represents the baseline hardness of the polymer matrix. PEEK is a high-performance thermoplastic polymer known for its excellent toughness, chemical resistance, and thermal stability; however, its hardness is comparatively lower than ceramic-reinforced composites. In the absence of reinforcing particles, the material undergoes relatively higher localized deformation when subjected to indentation during hardness testing. Furthermore, in 3D-printed polymer components, the existence of microscopic voids, layer boundaries, and incomplete fusion between deposited filaments can slightly reduce

the hardness performance of the printed structure [5-7]. When 3 wt.% nHA is added to the PEEK matrix, the hardness increases significantly to 67 VHN**.** This improvement indicates that the incorporation of nano-hydroxyapatite enhances the resistance of the composite against plastic deformation. The increase in hardness can be attributed to the intrinsic hardness and stiffness of hydroxyapatite particles, which act as rigid reinforcement within the softer polymer matrix. The uniformly dispersed nanoparticles restrict the movement of polymer chains and improve the load-bearing capability of the composite surface. Additionally, the strong interfacial bonding between PEEK and nHA facilitates efficient stress transfer during indentation, thereby increasing the overall hardness of the material. Further increasing the reinforcement concentration to 6 wt.% nHA results in a hardness value of 75 VHN, showing a continued improvement in surface strength and rigidity. At this concentration, the nanoparticles are likely well dispersed within the matrix, leading to enhanced reinforcement efficiency. The increased ceramic content strengthens the composite structure by reducing localized deformation under the indenter. In addition, the presence of nano-hydroxyapatite particles contributes to improved resistance against wear and surface damage. From the perspective of 3D printing, optimized filler loading may also improve the dimensional stability and interlayer bonding of the printed material by enhancing heat distribution during filament deposition. Better interlayer adhesion minimizes weak regions within the printed structure, thereby contributing to higher hardness values. The maximum hardness value of 81 VHNis obtained at 9 wt. % nHA, indicating that increasing ceramic reinforcement continuously improves the hardness of the composite. Unlike tensile or impact properties, hardness generally benefits from higher ceramic filler content because hydroxyapatite particles possess inherently high rigidity and resistance to indentation. The increased amount of nHA reduces the mobility of the polymer matrix and increases the stiffness of the composite surface. As a result, the material exhibits greater resistance to indentation and surface deformation. Moreover, the higher ceramic content enhances the compactness of the composite microstructure, which further contributes to increased hardness. The improvement in hardness with increasing nHA content can also be associated with the effects of the 3D-printing process. In fused filament fabrication or similar additive manufacturing techniques, processing parameters such as nozzle temperature, raster orientation, layer thickness, and cooling rate influence the micro structural integrity of the printed composite. The addition of nHA particles may improve thermal stability and reduce shrinkage during printing, leading to improved layer fusion and reduced porosity [11-13]. A denser and more compact printed structure enhances the hardness performance of the final component. However, excessive filler loading beyond the investigated range could potentially cause particle agglomeration and poor printability, which may eventually affect the uniformity of the material. Overall, the graph clearly demonstrates that the incorporation of nano-hydroxyapatite significantly improves the Vickers hardness of 3D-printed PEEK-LT3 composites. The hardness increases steadily from 55 VHN for pure PEEK-LT3 to 81 VHN at 9 wt. % nHA, indicating substantial enhancement in surface strength and resistance to deformation. The improvement is mainly attributed to the high stiffness of hydroxyapatite particles, enhanced interfacial bonding, restricted polymer chain mobility, and improved micro structural integrity produced during the 3D-printing process. Therefore, the addition of nHA reinforcement is highly effective in enhancing the hardness and wear resistance of the developed PEEK-based composite system [14].

3.4 MICRO STRUCTURE.

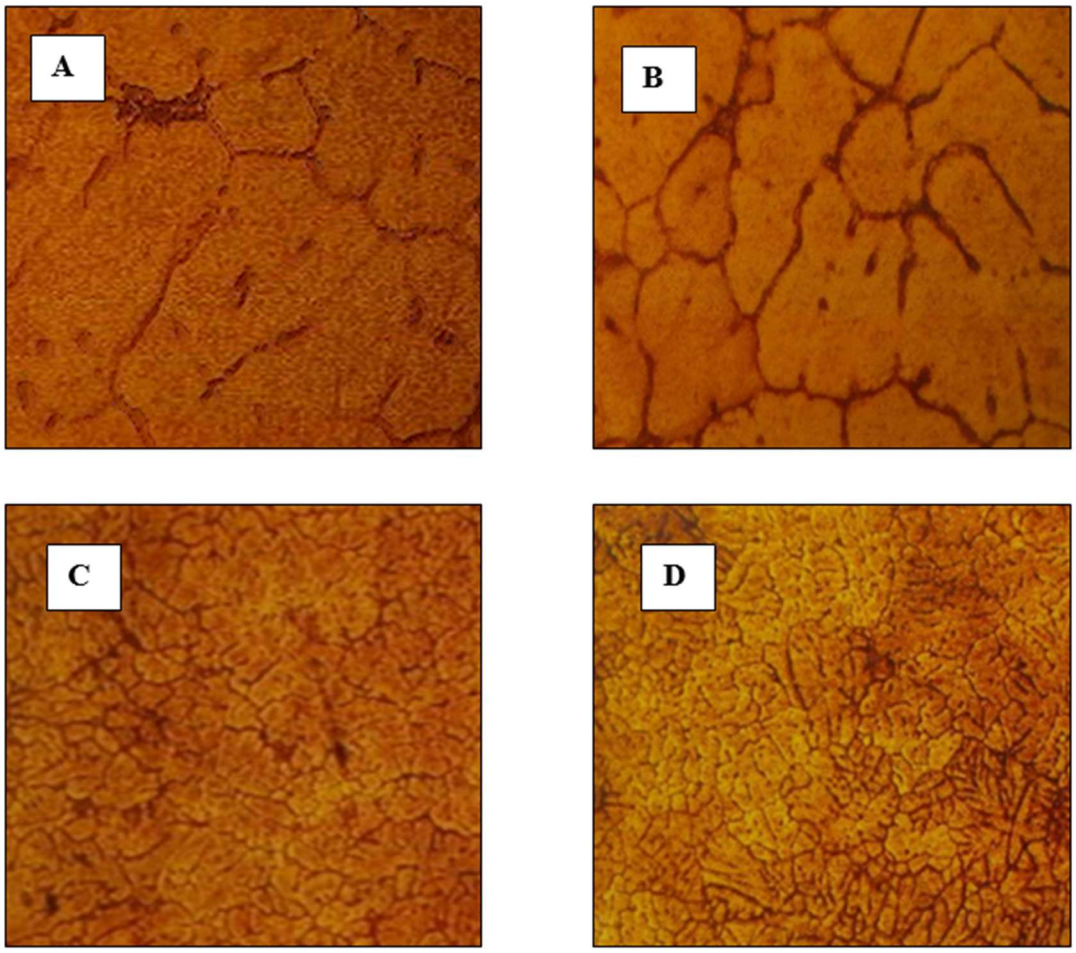

Fig 3.4 : Microscopic view of specimen a) PEEK-LT3-0%Wt nHA b) PEEK-LT3-3%Wt nHA c) PEEK-LT3-6%Wt nHA d) PEEK-LT3-9%Wt nHA

The microstructure of the hybrid composites was examined using an optical microscope (Model: Olympus), and a scanning electron microscope (SEM). JSM-6610LV scanning electron microscope equipped with energy dispersive X-ray analyzer (EDX) was used to study microstructure of the hybrid composites. The samples of unreinforced and hybrid composites for SEM were cut from tensile specimens and ground by means of abrasive papers followed by rotating disk cloth polishing. Keller's reagent (95ml water, 2.5ml HNO3, 1.5ml HCl, 1.0ml HF). The optical micrographs presented in Figure 3.4 show the micro structural evolution of PEEK-LT3 and its carbon-fiber-reinforced composites at different reinforcement levels of 0%, 3%, 6%, and 9% nHA [41].

In Image A, corresponding to neat PEEK-LT3 (0% nHA), the microstructure appears homogeneous with a continuous polymer matrix and smooth boundaries, reflecting the ductile nature of the material but also explaining its relatively low tensile strength and hardness [38]. Image B, representing the composite with 3% nHA, reveals the presence of dispersed reinforcement with regions of clustering and dark boundaries that disrupt matrix continuity. These irregularities act as stress concentrators, which reduce impact resistance and limit the improvement in tensile properties. In Image C, corresponding to 6% nHA, the fibers appear more uniformly distributed with better bonding at the fiber–matrix interface and fewer voids. These irregularities act as stress concentrators, which reduce impact resistance and limit the improvement in tensile properties. In Image C, corresponding to 6% nHA, the fibers appear more uniformly distributed with better bonding at the fiber–matrix interface and fewer voids.

These irregularities act as stress concentrators, which reduce impact resistance and limit the improvement in tensile properties. In Image C, corresponding to 6% nHA, the fibers appear more uniformly distributed with better bonding at the fiber–matrix interface and fewer voids. This improved homogeneity and load transfer efficiency and crack-arresting ability, which correlates with the peak

tensile strength and significant increase in hardness observed for this composition, making it the optimum reinforcement level. Finally, Image D, corresponding to 9% nHA, shows a denser fiber network with some signs of agglomeration and micro void formation. While the higher reinforcement level contributes to improved hardness and wear resistance, the presence of clusters reduces ductility and introduces brittleness, leading to a slight decline in tensile and impact properties compared to the 6% nHA composition.

3.5 SEM.

The scanning electron micrographs of PEEK-LT3 and its carbon fiber-reinforced composites at different fiber loadings reveal distinct morphological features that correlate well with the observed mechanical properties [9]. In the case of neat PEEK-LT3 (0% nHA), the microstructure appears relatively smooth and homogeneous, with no reinforcing elements visible. This matrix-dominated morphology explains the lower tensile strength and hardness, while the absence of rigid fillers allows the polymer to retain higher ductility and impact resistance. At 3% carbon fiber reinforcement, the SEM image shows the presence of fiber fragments partially embedded within the matrix, but also reveals interfacial voids and evidence of fiber pull-out [21]. The non-uniform dispersion and localized clustering of fibers reduce effective stress transfer, which corresponds to only a moderate improvement in tensile strength and a decline in impact performance. A significant improvement is observed at 6% nHA, where the microstructure displays well dispersed fibers with improved adhesion to the matrix, fewer voids, and stronger interfacial bonding. The rough fracture surface and fractured fibers indicate effective load transfer and higher energy absorption, which is consistent with the peak tensile strength and hardness recorded at this reinforcement level [29].

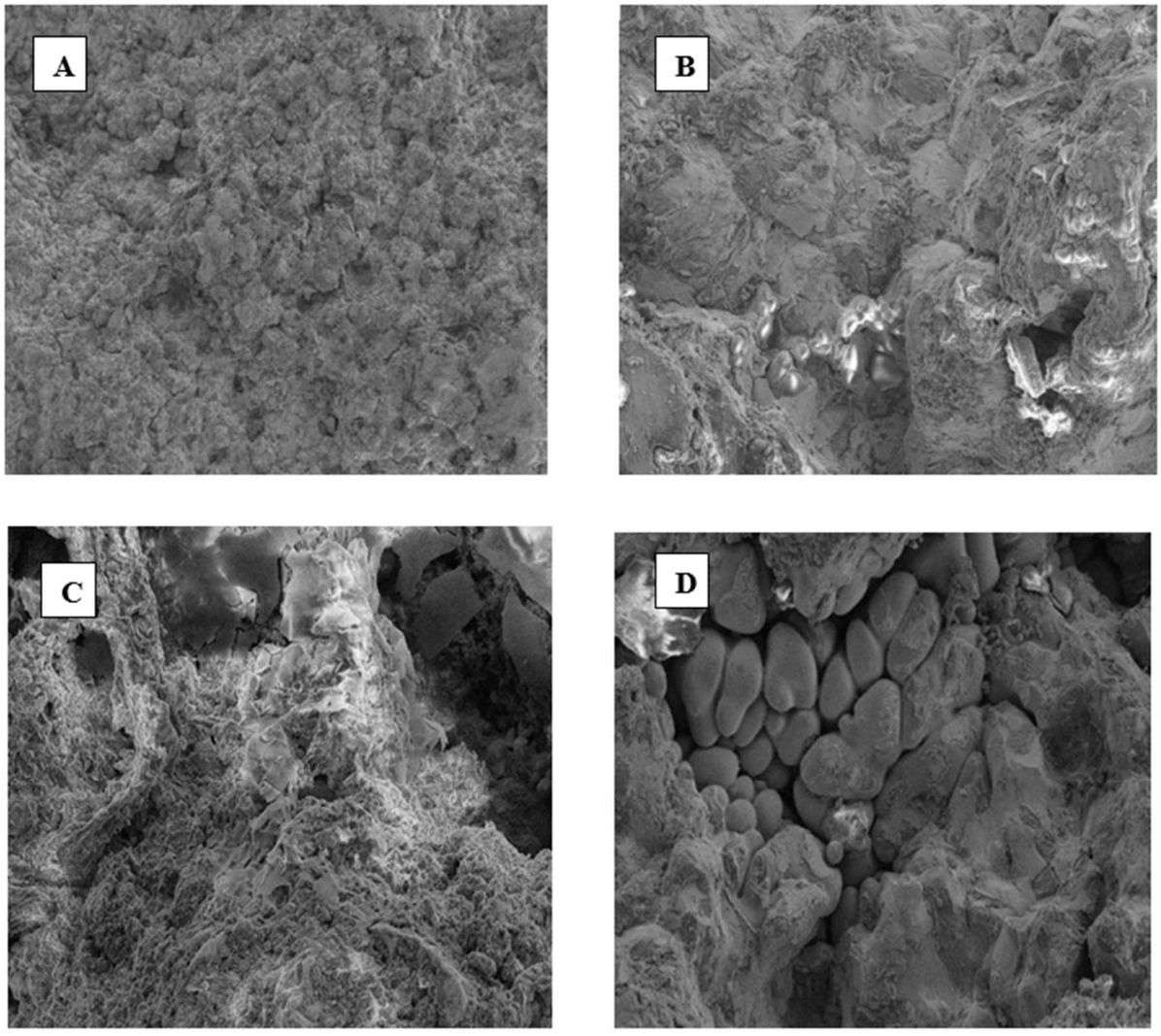

Fig 4.4: SEM Images. a) PEEK-LT3-0%Wt nHA b) PEEK-LT3-3%Wt nHA c) PEEK-LT3-6%Wt nHA d) PEEK-LT3-9%Wt nHA

However, at 9% nHA, the micrograph shows a dense concentration of fibers along with clear signs of agglomeration and micro void formation. Although hardness continues to improve due to the higher fiber content, the clustering and poor interfacial bonding reduce ductility and lead to a slight reduction in tensile and impact properties compared to the 6% nHA composition. Overall, the SEM analysis validates that uniform dispersion and strong interfacial bonding at 6% nHA yield the most balanced mechanical performance, while higher reinforcement levels increase brittleness despite improving hardness.

4. COCLUSION

PEEK-LT3/nHA composites were successfully fabricated using FDM-based 3D printing and evaluated for their mechanical and microstructural properties. The addition of nano-hydroxyapatite significantly enhanced the tensile strength, impact strength, and hardness of the composites. The optimum performance was achieved at 6 wt.% nHA, with a tensile strength of 277.66 MPa and impact strength of 44.5 kJ/m² due to improved interfacial bonding, uniform particle distribution, and better layer adhesion during printing. Hardness increased continuously with increasing nHA content, reaching 81 VHN at 9 wt.% nHA. SEM and microstructural analysis confirmed improved matrix–reinforcement interaction at optimum reinforcement levels, while higher filler loading caused agglomeration and increased brittleness. Overall, the developed 3D-printed PEEK-LT3/nHA composites demonstrated excellent potential for biomedical and lightweight structural applications.

5. REFERENCES

1. Bankole I. Oladapo, S. Abolfazl Zahedi, Sikiru O. Ismail, Francis T. Omigbodun, “3D Printing of PEEK-LT3 and Its Composite to Increase Biointerfaces as a Biomedical Material”, *Colloids and Surfaces B: Biointerfaces*, 203 (2021) 111726.
2. Pedro Rendas, Lígia Figueiredo, Madalena Geraldo, Catarina Vidal, B.A. Soares, “Improvement of Tensile and Flexural Properties of 3D Printed PEEK-LT3 Through the Increase of Interfacial Adhesion”, *Journal of Manufacturing Processes*, 93 (2023), 260–274.
3. Zhenzhen Wang and Yan Yang, “Application of 3D Printing in Implantable Medical Devices”, *BioMed Research International*, 2021, Article ID 6653967.
4. Ivan Vladislavov Panayotov, Valérie Orti, Frédéric Cuisinier, Jacques Yachouh, “Polyetheretherketone (PEEK-LT3) for Medical Applications”, *Journal of Materials Science: Materials in Medicine*, 27 (2016), 118.
5. Jianfeng Kang, Jibao Zheng, Yijun Hui and Dichen Li, “Mechanical Properties of 3D-Printed PEEK-LT3/HA Composite Filaments”, *Polymers*, 14 (2022), 4293.
6. Peng Wang, Bin Zou, Shouling Ding, Chuanzhen Huang, Zhenyu Shi, Yongsheng Ma, Peng Yao, “Preparation of Short NHA/GF Reinforced PEEK-LT3 Composite Filaments and Their Comprehensive Properties Evaluation for FDM-3D Printing”, *Composites Part B*, 2020.
7. Rupak Dua, Zuri Rashad, Joy Spears, Grace Dunn and Micaela Maxwell, “Applications of 3D-Printed PEEK-LT3 via Fused Filament Fabrication: A Systematic Review”, *Polymers*, 13 (2021), 4046.
8. Sunpreet Singh, Chander Prakash, Seeram Ramakrishna, “3D Printing of Polyether-Ether-Ketone for Biomedical Applications”, *European Polymer Journal*, 114 (2019), 234–248.
9. Ling Wang, Ziyu Wang, Jiayin Liu, Yijun Hui, “The Effects of Structural and Materials Design on the Mechanisms of Tissue Integration with the 3D Printed Polyether-Ether-Ketone Cranial Implants In Vivo”, *Additive Manufacturing Frontiers*, 3 (2024), 200112.
10. Benjamín Ortega-Bautista, John Henao, Carlos A. Poblano-Salas, Astrid L. Giraldo-Betancur, “Understanding the Deposition of Multilayered Hydroxyapatite-Bioactive Glass/Hydroxyapatite/Titanium Dioxide Coatings on PEEK-LT3 Substrates by Plasma Spray”, *Surface and Coatings Technology*, 494 (2024), 131543.
11. Xingting Han, Neha Sharma, Sebastian Spintzyk, Yongsheng Zhou, Zeqian Xu, “Tailoring the Biologic Responses of 3D Printed PEEK-LT3 Medical Implants by Plasma Functionalization”, *Dental Materials*, 38 (2022), 1083–1098.
12. Zhi Zheng, Pengjia Liu, Xingmin Zhang, Jingguo Xin, “Strategies to Improve Bioactive and Antibacterial Properties of Polyetheretherketone (PEEK-LT3) for Use as Orthopedic Implants”, *Materials Today Bio*, 16 (2022), 100402.
13. Jian-Wei Tseng, Chao-Yuan Liu, Yi-Kuang Yen, Johannes Belkner, “Screw Extrusion-Based Additive Manufacturing of PEEK-LT3”, *Materials & Design*, 140 (2018), 209–221.
14. Makena Mbogori, Abhishek Vaish, Raju Vaishya, Abid Haleem, Mohd Javaid, “Poly-Ether-Ether-Ketone (PEEK-LT3) in Orthopaedic Practice – A Current Concept Review”, *Journal of Orthopaedic Reports*, 1(1) (2022), 3–7.
15. Hongyun Ma, Angxiu Suonan, Jingyuan Zhou, Qiling Yuan, “PEEK-LT3 (Polyether-Ether-Ketone) and Its Composite Materials in Orthopedic Implantation”, *Arabian Journal of Chemistry*, 14(3) (2021), 102977.
16. Jibao Zheng, Jianfeng Kang, Changning Sun, Chuncheng Yang, “Effects of Printing Path and Material Components on Mechanical Properties of 3D-Printed Polyether-Ether-Ketone/Hydroxyapatite

Composites", *Journal of the Mechanical Behavior of Biomedical Materials*, 118 (2021), 104475.
17. Wenzhuo Zheng, Dongxu Wu, Yaowen Zhang, Yankun Luo, "Multifunctional Modifications of Polyetheretherketone Implants for Bone Repair: A Comprehensive Review", *Biomaterial Advances*, 154 (2023), 213607.
18. Xu Chen, Yanlong Wu, Huilong Liu, Yaning Wang, "Mechanical Performance of PEEK-LT3-Ti6Al4V Interpenetrating Phase Composites Fabricated by Powder Bed Fusion and Vacuum Infiltration Targeting Large and Load-Bearing Implants", *Materials & Design*, 215 (2022), 110531.
19. Prashant Jindal, Jogendra Bharti, Vipin Gupta, S.S. Dhami, "Mechanical Behaviour of Reconstructed Defected Skull with Custom PEEK-LT3 Implant and Titanium Fixture Plates Under Dynamic Loading Conditions Using FEM", *Journal of the Mechanical Behavior of Biomedical Materials*, 146 (2023), 106063.
20. Qing Zhang, Changning Sun, Jibao Zheng, Ling Wang, "Mechanical Behaviour of Additive Manufactured PEEK-LT3/HA Porous Structure for Orthopaedic Implants: Materials, Structures and Manufacturing Processes", *Journal of the Mechanical Behavior of Biomedical Materials*, 163 (2025), 106848.
21. Miaomiao He, Ce Zhu, Dan Sun, Zheng Liu, Meixuan Du, "Layer-by-Layer Assembled Black Phosphorus/Chitosan Composite Coating for Multi-Functional PEEK-LT3 Bone Scaffold", *Composites Part B*, 246 (2022), 110266.
22. Zilin Zhang, Xingmin Zhang, Zhi Zheng, Jingguo Xin, Song Han, "Latest Advances: Improving the Anti-Inflammatory and Immunomodulatory Properties of PEEK-LT3 Materials", *Materials Today Bio*, 22 (2023), 100748.
23. Beining Zhang, Siwei Lu, Jingyi Niu, Chuncheng Yang, "Influence of Reinforcement Phase Content on Mechanical Properties of Hydroxyapatite/Carbon Fiber/Polyether-Ether-Ketone Composites 3D Printed by Screw Extrusion", *Composites Science and Technology*, 258 (2024), 110843.
24. Houfeng Jiang, Ru Jia, Wurikaixi Aiyiti, Patiguli Aihemaiti, "Infill Strategies for 3D-Printed NHA-PEEK-LT3/HA-PEEK-LT3 Honeycomb Core-Shell Composite Structures", *Journal of Manufacturing Processes*, 92 (2023), 338–349.
25. Wenchao Li, Zhengnan Su, Yanru Hu, Lihui Meng, "Functional and Structural Construction of Photothermal-Responsive PEEK-LT3 Composite Implants to Promote Bone Regeneration and Bone-Implant Integration", *Journal of Manufacturing Processes*, 92 (2023), 338–349.
26. Zhimou Zeng, Linnan Wang, Bo Qu, Xingyu Gui, "Enhanced Osteogenesis and Inflammation Suppression in 3D Printed n-HA/PA66 Composite Scaffolds with PTH(1-34)-Loaded nPDA Coatings", *Composites Part B*, 282 (2024), 111566.
27. Debashish Gogoi, Manjesh Kumar, Jasvinder Singh, "A Comprehensive Review on Hydrogel-Based Bio-Ink Development for Tissue Engineering Scaffolds Using 3D Printing", *Annals of 3D Printed Medicine*, 15 (2024), 100159.
28. Shuai Li, Tianqi Wang, Shuai Chen, Yingze Li, "Compressive Properties and Biocompatibility of Additively Manufactured Lattice Structures by Using Bioactive Materials", *Thin-Walled Structures*, 205 (2024), 112469.
29. Qiujiang Li, Bowen Hu, Linan Wang, Lei Wang, "Biomineralized PEEK-LT3 Cages Containing Osteoinductive CaP Bioceramics Promote Spinal Fusion in Goats", *Bioactive Materials*, 45 (2025), 128–147.
30. Yanwen Su, Jiankang He, Nan Jiang, Hao Zhang, "Additively-Manufactured Poly-Ether-Ether-Ketone (PEEK-LT3) Lattice Scaffolds with Uniform Microporous Architectures for Enhanced Cellular Response and Soft Tissue Adhesion", *Materials & Design*, 191 (2020), 108671.
31. Jibao Zheng, Huiyu Zhao, Enchun Dong, Jianfeng Kang, "Additively-Manufactured PEEK-LT3/HA Porous Scaffolds with Highly-Controllable Mechanical Properties and Excellent Biocompatibility", *Materials Science and Engineering C*, (2021), 112333.
32. Jibao Zheng, Huiyu Zhao, Zhicong Ouyang, Xinying Zhou, "Additively-Manufactured PEEK-LT3/HA Porous Scaffolds with Excellent Osteogenesis for Bone Tissue Repairing", *Composites Part B*, 232 (2022), 109508.
33. Faisal Manzoor, Atefeh Golbang, Swati Jindal, Dorian Dixon, "3D Printed PEEK-LT3/HA Composites for Bone Tissue Engineering Applications: Effect of Material Formulation on Mechanical Performance and Bioactive Potential", *Journal of the Mechanical Behavior of Biomedical Materials*, 121 (2021), 104601.
34. Wenling Gao, Jintao Deng, Jianhua Ren, Wenhui Zhang, "3D-Printed Hydroxyapatite (HA) Scaffolds Combined with Exosomes from BMSCs Cultured in 3D HA Scaffolds to Repair Bone Defects", *Composites Part B*, 247 (2022), 110315.
35. Elena P. Ivanova, Kateryna Bazaka, Russell J. Crawford, "Metallic Biomaterials: Types and Advanced Applications", in *New Functional Biomaterials for Medicine and Healthcare*, 2014, pp. 121–147.
36. L. K. Tejhashwini, Arun Karthick Selvam, K. Preetham Sai, "3D Printing in Orthopedics and Healthcare Applications – A Review", *2024 Tenth*

International Conference on Bio Signals, Images, and Instrumentation (ICBSII), 2024.

37. A. H. Mir and M. S. Charoo, "Friction and Wear Characteristics of Polyetheretherketone (PEEK-LT3) – Review", *IOP Conference Series: Materials Science and Engineering*, 561 (2019), 012051.
38. Roberto Chavez, Andraez Navaez, "Design and Construction of Twin Screw Extruder for the Fabrication of Polymer Based Filament with High Metal Loads: An Alternative for Emerging Economies", *Journal of Southwest Jiaotong University*, 59(2), 2024.
39. W. Hufenbach, K. Kunze, "Sliding Wear Behaviour of PEEK-LT3-PTFE Blends", *Journal of Synthetic Lubrication*, 20(3), 2003, pp. 227–242.
40. Syed Zameer, "Mechanical and Tribological Behavior of Bio Polymer Matrix Composites for Biomedical Prosthesis Application", *Advanced Material Research Journal*.